This article has been accepted for publication in a future issue of this journal, but has not been fully edited. Content may change prior to final publication. Citation information: DOI 10.1109/TPWRS.2021.3137257, IEEE Transactions on Power Systems

Service Restoration for Resilient Distribution Systems Coordinated with Damage Assessment

Yiheng Bian, *Student Member, IEEE,* Chen Chen, Senior *Member, IEEE,* Yuxiong Huang, *Student Member, IEEE,* Zhaohong Bie, *Senior Member, IEEE,* and João P. S. Catalão, *Senior Member, IEEE*

***Abstract*—The time required to restore distribution systems following an extreme event is highly dependent on damage assessment. Waiting for field assessors patrolling the feeders to identify fault locations is a bottleneck in improving restoration efficiency. This paper proposes an optimal service restoration model for resilient distribution systems considering the coordination with damage assessment, as a contribution to earlier studies. The restoration actions such as fault isolation, network reconfiguration, crew mobilization and fault repair are brought forward to the damage assessment stage and the restoration schedules are dynamically updated with the reveal of the damage status. The relationship between fault location, switch status and node status is established to optimize the network topology and guarantee crew operation safety under the condition that the network has multiple faults or unchecked potential faulted areas. Moreover, the crew routing formulations are modified to enable fault isolation and load island reconnection by manual switches during the restoration process. Case studies validate the effectiveness of the proposed model in reducing load shedding and restoration duration.**

***Index Terms*—Distribution system, damage assessment, service restoration, reconfiguration, crew dispatch.**

NOMENCLATURE

Acronyms

CB	Circuit breaker
DER	Distributed energy resources
DG	Distributed generators
DN	Damaged component
DS	Distribution system
ESS	Energy storage systems
MS	Manual switch
MG	Microgrid
PV	Photovoltaic
RCS	Remote controlled switch

Indices and Sets

$\mathbf{T}_h$	Set of optimization time horizon at time step h
SP_c, RP_c	Indexes of start and return points for repair crew c
w, W	Index and set of depots for resources pick up
$\mathbf{V}$	Set of buses
$\mathbf{L}$	Set of distribution lines
$\mathbf{N}$	Set of manual switches, damaged components and depots for resources pick up
Sub	Set of substation nodes
Ω_G, Ω_{PV}, Ω_{ES}	Set of dispatchable DGs, PV systems and ESSs
DN	Set of damaged components
MS	Set of manual switches
MS^{open}, MS^{close}	Set of vertices representing the closed manual switches to be opened and the opened manual switches to be closed in the crew routing problem
c, $Crew$	Index and set of repair crews
$\pi(j)$, $\delta(j)$	Set of parent and child nodes of node j

Parameters

T_h	Optimization horizon duration at time step h
Δt	The time interval of each time step
N^V	Total number of distribution nodes
$\rho_{j,t}$	Priority of load at node j
r_{ij}, x_{ij}	Resistance/reactance of line (i, j)
$U^{\min}$, $U^{\max}$	Lower and upper bounds of allowed voltage
$S_{ij}^{\max}$	Maximum apparent power limit of line (i, j)
$P_j^{G,\max}$, $Q_j^{G,\max}$	Maximum active and reactive power output of dispatchable DG or substation j
$P_{j,t}^L$, $Q_{j,t}^L$	Active and reactive load of node j at time step t
$P_{j,t}^{PV}$	Active power output of PV generator j at time t
θ_j	Power factor of PV generator j
$P_j^{ch,\min}$ / $P_j^{dch,\min}$, $P_j^{ch,\max}$ / $P_j^{dch,\max}$	Minimum and maximum active charging / discharging power limits of ESS j
$Q_j^{ES,\min}$, $Q_j^{ES,\max}$	Minimum and maximum reactive power output of ESS j
$E_j^{ES,ini}$	Initial energy storage of ESS j
$E_j^{ES,\min}$, $E_j^{ES,\max}$	Minimum and maximum stored energy of ESS j
η_j^{ch}, η_j^{dch}	Charging and discharging efficiency coefficients
f_{ij}^{check}	Binary parameter equal to 1 if line (i, j) is checked by damage assessors
$t_{n,c}^{opera}$	Time for crew c to repair component n or operate manual switch n
$t_{n,c,m}^{travel}$	Traveling time for crew c from component /

This work was supported by the Science and Technology Project of State Grid, China under Grant SGJX0000KXJS1900322. *(Corresponding author: Zhaohong Bie.)*

Y. Bian, C. Chen, Y. Huang and Z. Bie, are with the State Key Laboratory of Electrical Insulation and Power Equipment, Shaanxi Key Laboratory of Smart Grid, Xi'an Jiaotong University, Xi'an 710049, China (e-mail: byh0xyz@stu.xjtu.edu.cn; morningchen@xjtu.edu.cn; hyx.xj@stu.xjtu.edu.cn; zhbie@mail.xjtu.edu.cn;).

J.P.S. Catalão is with the Faculty of Engineering of the University of Porto (FEUP) and INESC TEC, Porto 4200-465, Portugal (e-mail: catalao@fe.up.pt).

manual switch n to m

Cap_r^R Capacity required to carry one unit of resource r

Cap_c^C The maximum capacity of crew c

$\mathcal{R}_{m,r}$ The units number of type r resources required to repair damaged component m

$Res_{c,SP,r}^C$ The units number of type r resources that crew c obtains from the start point

$y_{ij\kappa}^{RCS}$ / $y_{ij\kappa}^{MS}$ Binary parameter equal to 1 if a remote-controlled switch / manual switch is placed at i side ($\kappa=1$) or j side ($\kappa=2$) of line (i, j)

ε , M A sufficient small / large positive number

Variables

$P_{ij,t}$, $Q_{ij,t}$ Active and reactive power flow at the distribution line from node i to j at time step t

$P_{j,t}^G$, $Q_{j,t}^G$ Active and reactive power output of dispatchable DG or substation j at time step t

$Q_{j,t}^{PV}$ Reactive power output of PV unit j at time t

$P_{j,t}^{ch}$, $P_{j,t}^{dch}$ Active power charge and discharge of ESS j at time step t

$Q_{j,t}^{ES}$ Reactive power output of ESS j at time step t

$u_{j,t}^{ch}$ / $u_{j,t}^{dch}$ Binary variable equal to 1 if ESS j operates in the charging / discharging mode at time step t

$E_{j,t}^{ES}$ Energy storage of ESS j at time step t

$U_{j,t}$ Voltage magnitude of node j at time step t

$B_{ij,t}$ Binary variable equal to 1 if line (i, j) is faulted or is not checked at time step t

$c_{ij,t}$ Binary variable equal to 1 if the status of line (i, j) is on at time step t

$En_{j,t}^L$ Binary variable equal to 1 if load at node j is picked up at time step t

$En_{j,t}^G$ Binary variable equal to 1 if the dispatchable DG or substation at node j is energized at time step t

$En_{j,t}^{PV}$ / $En_{j,t}^{ES}$ Binary variable equal to 1 if the PV unit/ ESS at node j is energized at time step t

$x_{j,t}$ Binary variable equal to 1 if node j is influenced by outage propagation at time step t

$\gamma_{j,t}$ Binary variable equal to 1 if node j is chosen as a root node at time step t

$F_{ij,t}$ / $F_{ij,t}^f$ / $F_{ij,t}^G$ Fictitious power flow from node i to j at time step t used to determine the island connectivity / outage propagation status / DERs energization status

$W_{j,t}$ Fictitious power output of node j at time step t

$y_{ij1,t}$ / $y_{ij2,t}$ Binary variable equal to 1 if the switch at i/ j side of line (i, j) is closed at time step t or the line is non-switchable

$f_{ij\kappa,t}^{MS,open}$ / $f_{ij\kappa,t}^{MS,close}$ Binary variable equal to 1 if manual switch at i side ($\kappa=1$) or j side ($\kappa=2$) of line (i, j) is opened / closed at time step t

$f_{n,t}^{fix}$ Binary variable equal to 1 if damaged component n is brought into normal status at time step t

$X_{m,c,n}$ Binary variable equal to 1 if the travel path of crew c is from component or manual switch m to n

$\tau_{n,c}$ Binary variable equal to 1 if component or manual switch n is repaired/operated by crew c

$t_{n,c}^{arrive}$ Time when crew c arrives at component or manual switch n

$t_{n,c}^{start}$ Time when crew c start the repair or operation of component / manual switch n

$E_{c,m,r}$ The units number of type r resources that crew c has before repairing damaged component m

$Res_{c,w,r}^C$ The units number of type r resources that crew c picks up from depot w

I. Introduction

In the last decades, the increasingly frequent extreme events, such as hurricanes, ice storms and floods, have imposed sever impacts on power systems [1]. There is an urgent requirement to boost power system resilience, i.e. enhance the ability of power systems to resist, adapt to and efficiently recover from such extreme events [2]. Distribution systems (DSs) are closely related to customer load service and more vulnerable to extreme events. Improving the DS outage management and expediting service restoration are critical ways to reduce power outages and mitigate economic losses. The increasing penetration of distributed energy resources (DERs) including dispatchable distributed generators (DGs), photovoltaic (PV) systems, energy storage systems (ESSs), etc. provides backup power sources during a major outage. Moreover, with the emerging smart grid technologies, it is possible to actively improve DS resilience by advanced measures such as network reconfiguration and microgrids (MGs) formation. Ref. [3-6] exploit DGs and remote controlled switches (RCSs) or manual switches (MSs) to form multiple MGs in the DS to restore the load after major faults while maintaining the radial structure.

A key task for DS restoration is to schedule and route repair crews to efficiently repair the faults after disasters. The co-optimization of crew routing and network reconfiguration for service restoration is studied in [7]. The authors in [8] expanded the co-optimization model by incorporating mobile power source dispatch into DS restoration. One concern to be addressed in the above literatures is that they assume the RCS is equipped at each distribution line so that the fault is isolated within the line segment, which is neither economical nor affordable in most cases [9]. In [10], the authors proposed a resilience-oriented strategy for DS planning problem. RCSs are only deployed at the selected lines and a fictitious network is designed to model the outage propagation in the network until RCSs disconnect lines. Authors in [11] studied the dispatch of tree and line crews and modeled fault isolation for the restoration of DS. In addition, the operation of MSs performed by qualified crews on the scene is also a considerable operation during DS restoration. Ref. [12] introduced a synthetic restoration model for DSs to determine the switching and energization sequence considering the coordination of crew dispatch and RCS/MS operation.

In the perspective of the overall restoration process for DSs after extreme events, service restoration is considered as one step performed after information collection and damage assessment [13]. More specifically, to make preparation for the subsequent restoration, firstly the outage management system (OMS) will receive the information from multiple sources like field measurements, smart meters and trouble call systems to

primarily analyze the damage status [14-16], and then the field checkers are dispatched to precisely locate the fault and estimate the damage extent and resources needed for restoration [17]. The duration of damage assessment, especially the time spent on the field checker patrol, impacts the length and cost of the overall restoration effort. However, existing literatures usually assume a separation of damage assessment and service restoration, which restricts the restoration effect. Ref. [18] indicated that an online stochastic optimization for joint assessment and restoration provides high-quality solutions to the restoration problem. Ref. [19] discussed the emergency repair mode in which crews patrol the possible faulted branch lines after repairing the skeleton network. Moreover, the restoration cases of the power grids in China's southeast coastal provinces in response to typhoon shows that starting the repair as soon as partial information of damage is revealed is also a common practice under emergency conditions.

In this paper, we propose a service restoration model for DSs considering the coordination with damage assessment. After partial network is checked by damage assessors, service restoration is conducted according to the gradual reveal of uncertainties. The restoration measures include isolating the faults to narrow down the interrupted parts, restoring the non-fault parts through reconfiguration and MGs formation, repairing the faults and reconnecting the repaired parts. There are several challenges to consider the overall restoration process: 1) fault isolation, reconfiguration, MGs formation and load island reconnection should be integrated in an optimization problem, and a mechanism which coordinates these measures with damage assessment should be designed; 2) A topology optimization method capable of isolating multiple faults or unchecked potential faulted areas is required to restore load and guarantee crew safety; 3) the crew operating MSs to isolate faults and reconnect the repaired parts should be considered in crew routing formulations.

This paper puts forward the solutions of the above challenges and provides the following contributions:

1) A novel restoration model is proposed from the view of overall restoration process to overcome the obstacles caused by the separation of damage assessment and service restoration and further improve DS restoration efficiency. A coordination mechanism is designed to restore the system as the damage assessment progresses.

2) The relationship between fault location, switch status and node status is established, which is used to optimize the network topology in the case of multiple faults / unchecked potential faulted areas exist and guarantee crew safety during repair and MS operation.

3) The crew routing formulations are expanded to incorporate both the open and close operation of MSs to enable fault isolation and load island reconnection during the whole restoration process.

The rest of this paper is organized as follows. Section II states the overall DS restoration process and model framework. Section III develops the mathematical formulation. Section IV provides numerical results to validate the proposed model. Conclusions and future work are discussed in Section VI.

II. Model Statement

A. Multi-stage restoration for DSs

A multi-stage DS restoration process summarized from [13, 19] is illustrated in Fig. 1. An extreme event occurs at t_1. The circuit breakers (CBs) or reclosers may trigger to isolate downstream feeders with sustained faults and maintain power supply for some customers [21]. Multisource information is collected during [t_2, t_3] to identify the potential faulted areas. Then damage assessment is carried out from t_3 to t_5 to precisely locate the faults and evaluate the damage extent and required resources. After some faults are identified in the course of damage assessment, RCSs can be used for fault isolation and pre-restoration [20]. This step is performed in time interval [t_4, t_5]. The repair crew departs from the utility at the end of damage assessment, i.e. t_5, and arrive on scene at t_6. Then, repair and switching are implemented until the end of restoration.

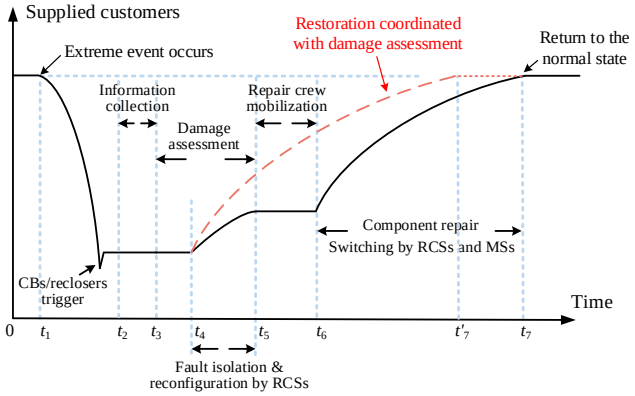

Fig. 1. Multi-stage restoration process for distribution systems

However, the separation of damage assessment and restoration is not necessarily the case in practice [18], [19]. Through bringing the restoration measures forward, the restoration effect is further improved and the interruption time is reduced, which is qualitatively shown by the red dashed line in Fig. 1.

B. Restoration coordinated with damage assessment

In this part, the framework of the proposed restoration model is described. It is assumed that the repair crew is responsible for repairing damaged components and operating MSs. The operation time of RCSs and CBs is assumed to be 0 for simplicity.

A simple feeder deployed with CB, RCS and MS is used to show the proposed coordination mechanism. As depicted in Fig. 2, after identifying the fault signal, CB triggers and DG is de-energized. The part downstream the CB is regarded as a potential faulted area. All loads are curtailed due to the disconnection with power sources at t=t_0 and they are marked in red. As the damage assessors patrol the potential faulted area, the damage status is gradually revealed and the repair crew routing decision is made dynamically through rolling horizon optimization. At time step t=t_1, line L3-4, L4-5 are checked and a fault at L3-4 is identified. The repair crew is dispatched to repair the fault and then open MS at L3-4 to isolate potential faults. After that, DG can be reconnected to restore load 4 and 5. At t=t_2, all potential fault sections are checked and a fault on L2-3 is found. RCS at L1-2 is opened to restore load 1. The

This article has been accepted for publication in a future issue of this journal, but has not been fully edited. Content may change prior to final publication. Citation information: DOI 10.1109/TPWRS.2021.3137257, IEEE Transactions on Power Systems

decision is updated again and the restoration measures are implemented according to the latest decision.

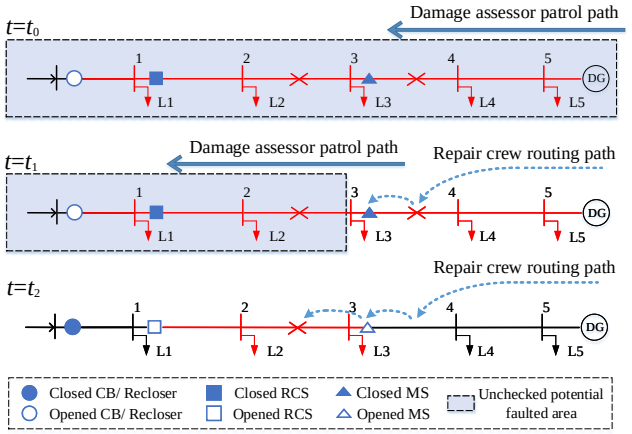

Fig. 2. A simple example for the coordination mechanism

Some remarks regarding the model framework are provided:

Remark 1: *the potential faulted area*. The collected multisource information is helpful to primarily pinpoint the faulted areas. However, data from fault-indicating devices and smart meters after an extreme event may be unavailable or questionable [13]. Moreover, faulted line section identification for multiple-fault scenarios remains a challengeable question. In this paper, we consider the parts downstream the triggered CBs as potential faulted areas and the uncertainty is only revealed by damage assessors.

Remark 2: *the routing path of damage assessors*. We set the travel path and patrol time of damage assessors as parameters and optimize service restoration decisions based on the dynamically updated parameters. The routing path of damage assessors can be determined with the objective of minimizing overall inspection time [22] or according to the expert experience. Determining it is out of the scope of this paper.

Remark 3: *task assignment of MS operation*. The MS can be operated by damage assessors to isolate the fault. In this paper, we assume the MS is only operated by the repair crew for the reason that damage assessment can be performed by unmanned aerial vehicles and fault isolation switching can be optimized when multiple faults and DGs exist. The proposed model can accommodate the case where damage assessors operate MSs by adjusting the initial switch status.

Remark 4: *crew safety guarantee*. To ensure crew safety when repairing damaged components and operating switches, for a node or line, if at least one connected path exists between it and a fault or potential faulted area, the node or line should be de-energized. A binary variable $x_{j,t}$ is introduced to indicate whether there is a connected path between node *j* and potential faults. Constraints are imposed to prevent the node with $x_{j,t}=1$ being connected to an operative power source.

III. Mathematical Formulation

The objective function is to maximize load restoration during the scheduling time horizon considering load priority:

$$\max \sum_{t\in\mathbf{T}_h}\Delta t\sum_{j\in\mathbf{V}}\rho_{j,t}En^L_{j,t}P^L_{j,t}-\alpha\sum_{t\in\mathbf{T}_h}\left(f^{MS,open}_{ij1,t}+f^{MS,open}_{ij2,t}+f^{MS,close}_{ij1,t}+f^{MS,close}_{ij2,t}\right) \quad (1)$$

where the first term indicates the total restored load considering the priority. The second term denotes total MS switching times with a small weight α. The second term is used to avoid unnecessary MS operation.

A. Operational Constraints

The DS operational constraints are formulated based on the linearized DistFlow model [23]. Specifically, Eq. (2)-(5) represent the constraints of nodal power balance, branch flow and voltage magnitude. Constraint (6) ensures DG output is limited by the capacity. The PV unit is assumed to operate at a constant power factor [24] and its reactive power output is determined using constraint (7). The charging and discharging power of ESSs is limited by constraint (8). Constraint (9) represents the relationship between charging/discharging power and the stored energy and sets the allowable range of energy storage for ESSs.

$$\begin{cases}\sum_{s\in\delta(j)}P_{js,t}-\sum_{i\in\pi(j)}P_{ij,t}=P^G_{j,t}+En^{PV}_{j,t}P^{PV}_{j,t}+P^{dch}_{j,t}-P^{ch}_{j,t}-En^L_{j,t}P^L_{j,t}\\ \sum_{s\in\delta(j)}Q_{js,t}-\sum_{i\in\pi(j)}Q_{ij,t}=Q^G_{j,t}+Q^{PV}_{j,t}+Q^{ES}_{j,t}-En^L_{j,t}Q^L_{j,t}\end{cases},\forall j\in\mathbf{V},\forall t \quad (2)$$

$$\begin{cases}U_{i,t}-U_{j,t}-(r_{ij}P_{ij,t}+x_{ij}Q_{ij,t})/U_0\le M(1-c_{ij,t})\\ U_{i,t}-U_{j,t}-(r_{ij}P_{ij,t}+x_{ij}Q_{ij,t})/U_0\ge -M(1-c_{ij,t})\end{cases},\forall(i,j)\in\mathbf{L},\forall t \quad (3)$$

$$\begin{cases}-S^{\max}_{ij}c_{ij,t}\le P_{ij,t}\le S^{\max}_{ij}c_{ij,t}\\ -S^{\max}_{ij}c_{ij,t}\le Q_{ij,t}\le S^{\max}_{ij}c_{ij,t}\\ -\sqrt{2}S^{\max}_{ij}c_{ij,t}\le P_{ij,t}+Q_{ij,t}\le -\sqrt{2}S^{\max}_{ij}c_{ij,t}\\ -\sqrt{2}S^{\max}_{ij}c_{ij,t}\le P_{ij,t}-Q_{ij,t}\le -\sqrt{2}S^{\max}_{ij}c_{ij,t}\end{cases},\forall(i,j)\in\mathbf{L},\forall t \quad (4)$$

$$U^{\min}_j\le U_{j,t}\le U^{\max}_j\quad,\forall j\in\mathbf{V},\forall t \quad (5)$$

$$\begin{cases}0\le P^G_{j,t}\le En^G_{j,t}P^{G,\max}_j\\ 0\le Q^G_{j,t}\le En^G_{j,t}Q^{G,\max}_j\end{cases}\quad\forall j\in\mathbf{V},\forall t \quad (6)$$

$$Q^{PV}_{j,t}=En^{PV}_{j,t}P^{PV}_{j,t}\tan\left(\cos^{-1}\theta_j\right)\quad\forall j\in\mathbf{V},\forall t \quad (7)$$

$$\begin{cases}u^{ch}_{j,t}+u^{dch}_{j,t}\le En^{ES}_{j,t}\\ u^{ch}_{j,t}P^{ch,\min}_j\le P^{ch}_{j,t}\le u^{ch}_{j,t}P^{ch,\max}_j\\ u^{dch}_{j,t}P^{dch,\min}_j\le P^{dch}_{j,t}\le u^{dch}_{j,t}P^{dch,\max}_j\\ En^{ES}_{j,t}Q^{ES,\min}_j\le Q^{ES}_{j,t}\le En^{ES}_{j,t}Q^{ES,\max}_j\end{cases}\quad\forall j\in\mathbf{V},\forall t \quad (8)$$

$$\begin{cases}E^{ES}_{j,t}=E^{ES,ini}_j\ ,\ t=0\\ E^{ES}_{j,t}=E^{ES}_{j,t-1}+\Delta t\left(\eta^{ch}_jP^{ch}_{j,t}-\frac{1}{\eta^{dch}_j}P^{dch}_{j,t}\right),\forall t\in\mathbf{T}_h\quad\forall j\in\mathbf{V}\\ E^{ES,\min}_j\le E^{ES}_{j,t}\le E^{ES,\max}_j,\forall t\end{cases} \quad (9)$$

B. Constraints for Radial Topology

During restoration, fault is isolated and dynamic MGs are formed by operating switches. According to the graph theory, the graph is radial if and only if the following two conditions are satisfied: 1) each sub-graph is a connected graph; 2) the number of branches equals to the number of nodes minus the number of sub-graphs. The single-commodity flow method is adopted to model the radial topology constraints [25]. To ensure the connectivity of sub-graphs, a fictitious network is constructed. For each sub-graph, a "root node" is set to act as fictitious power source while other nodes are load nodes with a fictitious unit load demand. Then the graph connectivity is satisfied if at least one path exists between each load node and the root node. The radial structure is guaranteed by (10)-(13).

$$\gamma_{j,t}\le\sum_{i\in\pi(j)\cup\delta(j)}(1-c_{ij,t})\quad,\forall j\in\mathbf{V},\forall t \quad (10)$$

$$-M\gamma_{j,t}-1\le\sum_{s\in\delta(j)}F_{js,t}-\sum_{i\in\pi(j)}F_{ij,t}\le M\gamma_{j,t}-1,\quad\forall j\in\mathbf{V}\setminus Sub\ ,\forall t \quad (11)$$

This article has been accepted for publication in a future issue of this journal, but has not been fully edited. Content may change prior to final publication. Citation information: DOI 10.1109/TPWRS.2021.3137257, IEEE Transactions on Power Systems

$$-Mc_{ij,t} \le F_{ij,t} \le Mc_{ij,t} \quad ,\forall (i,j) \in \mathbf{L}, \forall t \tag{12}$$

$$\sum_{ij \in \mathbf{L}} c_{ij,t} = N^V - |Sub| - \sum_{j \in \mathbf{V}} \gamma_{j,t} \quad ,\forall t \tag{13}$$

In view of the fact that MGs or load islands are created by disconnecting lines, we regard the two nodes at the ends of a disconnected line as potential root nodes [26]. Constraint (10) indicates node j can be a root node if at least one of its linked line is disconnected. Eq. (11) is the power balance constraint for the fictitious network. It means that, for each node except the substation, it should be either a root node with unlimited power output ($\gamma_{j,t}=1$ to relax the constraint) or a load node with a unit demand ($\gamma_{j,t}=0$). Constraint (12) prevents fictitious power flowing on a disconnected line. Constraint (13) states the number of lines is equal to the number of nodes minus the number of substations and root nodes.

C. Constraints for node, line and switch status

If the switch at each side of a line is closed or the line is non-switchable, i.e. the line is not equipped with a switch, this line is connected. Otherwise it is disconnected, as expressed by (14).

$$\varepsilon\left(2-y_{ij1,t}-y_{ij2,t}\right) \le 1-c_{ij,t} \le M\left(2-y_{ij1,t}-y_{ij2,t}\right) \quad \forall (i,j) \in \mathbf{L}, \forall t \tag{14}$$

The following part establishes the relationship between the fault location, switch status and node status.

Once a fault occurs on a line, power outage will propagate to nodes connected to the line until the nearest switches isolate it [10]. The parts connected to the fault will remain interrupted until the fault is cleared. Take line (i, j) and node j as an example; as depicted in Fig. 3, node j will be influenced by outage propagation from line (i, j) under the following two scenarios. Scenario A: the fault occurs on line (i, j) and there is no switch to isolate the outage or the switch is closed at j side of the line ($B_{ij,t}=1$, $y_{ij2,t}=1$). Scenario B: node i is influenced by outage propagation and there is no switch or the switch is closed at either side of line (i, j) ($x_{j,t}=1$, $y_{ij1,t}=y_{ij2,t}=1$).

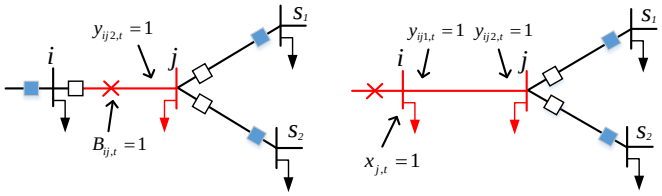

(a) Scenario A (b) Scenario B

Fig. 3. Scenarios where node j is influenced by outage propagation from (i, j)

Node j will be influenced by outage propagation if at least one connected line satisfies the characteristics of scenario A or B. The constraint can be listed as follows.

$$\begin{cases} Mx_{j,t} \ge \sum_{i \in \pi(j)} y_{ij2,t} \cdot B_{ij,t} + \sum_{s \in \delta(j)} y_{js1,t} \cdot B_{js,t} \\ Mx_{j,t} \ge \sum_{i \in \pi(j)} y_{ij1,t} \cdot y_{ij2,t} \cdot x_{i,t} + \sum_{s \in \delta(j)} y_{js1,t} \cdot y_{js2,t} \cdot x_{s,t} \end{cases} \quad \forall j \in \mathbf{V}, \forall t \tag{15}$$

The upper equation of (15) is corresponding to scenario A, which denotes if at least one line is faulted and there is no switch in the open status at the j side of the line, then node j should be influenced by outage ($x_{j,t}=1$). The lower equation is corresponding to scenario B, i.e. if at least one adjacent node of node j is influenced by the outage and the intermediate line has no switch in open status to isolate outage propagation, node j will be influenced by the outage ($x_{j,t}=1$).

On the other hand, if line (i, j) and node j is not belonging to scenario A∪B, node j should not be influenced by outage propagation from the path of line (i, j). Fig. 4 shows three scenarios which form a mutually exclusive set of A∪B. Scenario C: the switch at j side of line (i, j) is opened. Scenario D: there is an opened switch at i side of line (i, j) and no fault occurs on line (i, j). Scenario E: node i is not influenced by the outage and no fault occurs on line (i, j).

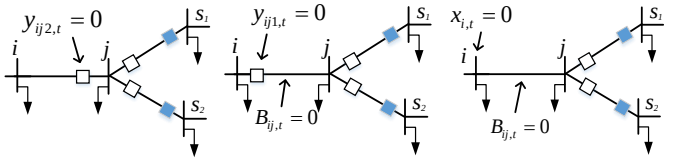

(a) Scenario C (b) Scenario D (c) Scenario E

Fig. 4. Scenarios where node j is not influenced by outage propagation from the path of line (i, j)

If all nodes and lines in a connected graph belong to C∪D∪E, the nodes in the graph should not be influenced by outage propagation, i.e. $x_{j,t}=0$. Similar to Section B, a fictitious network is constructed to identify whether there is an interrupted node in the connected graph where node j resides.

$$-M\left(\sum_{i \in \pi(j)} y_{ij2,t} \cdot B_{ij,t} + \sum_{s \in \delta(j)} y_{js1,t} \cdot B_{js,t}\right) \le W_{j,t} \le M\left(\sum_{i \in \pi(j)} y_{ij2,t} \cdot B_{ij,t} + \sum_{s \in \delta(j)} y_{js1,t} \cdot B_{js,t}\right) \quad \forall j \in \mathbf{V}, \forall t \tag{16}$$

$$\sum_{s \in \delta(j)} F^f_{js,t} - \sum_{i \in \pi(j)} F^f_{ij,t} = W_{j,t} - x_{j,t} \quad ,\forall j \in \mathbf{V}, \forall t \tag{17}$$

$$-Mc_{ij,t} \le F^f_{ij,t} \le Mc_{ij,t} \quad ,\forall (i,j) \in \mathbf{L}, \forall t \tag{18}$$

where $W_{j,t}$ denotes the fictitious power output from an interrupted node. Constraint (16) sets $W_{j,t}$ as 0 if all connected lines of node j belongs to C∪D∪E. Constraints (17) ensures $x_{j,t}=1$ only if the fictitious unit load can be served by a fictitious power source, i.e. there is at least one path between node j and an interrupted node. Otherwise, $x_{j,t}=0$. Constraint (18) limits fictitious power flow on a disconnected line to be 0.

Scenarios A to E include all possible ways in which power outage affects the node through the connected lines. Therefore constraints (15)-(18) strictly determine the status of each node in the network if switches status and the locations of multiple faults are given. A description is provided in Appendix to show the completeness of the scenarios.

D. Energization Status of DERs

The dispatchable DG and substation influenced by power outage propagation should be disconnected. Moreover, for the node without a controllable generator, the relevant energization status variable is set as 0.

$$En^G_{j,t} \le \left(1-x_{j,t}\right) \quad ,\forall j \in \mathbf{V}, \forall t \tag{19}$$

$$En^G_{j,t} = 0 \quad ,\forall j \in \mathbf{V} \setminus \{\Omega_G \cup Sub\}, \forall t \tag{20}$$

For PVs and ESSs, we assume they can connect to the system only if at least one energized controllable generator is in the same island to control the voltage and frequency [27]. To judge the connection between each node and a controllable generator, another fictitious network is constructed. The energization status of PVs and ESSs are represented by (21) and (22).

This article has been accepted for publication in a future issue of this journal, but has not been fully edited. Content may change prior to final publication. Citation information: DOI 10.1109/TPWRS.2021.3137257, IEEE Transactions on Power Systems

$$-M\cdot En_{j,t}^{G}-\left(En_{j,t}^{PV}+En_{j,t}^{ES}\right)\le \sum_{s\in\delta(j)}F_{js,t}^{G}-\sum_{i\in\pi(j)}F_{ij,t}^{G} \le M\cdot En_{j,t}^{G}-\left(En_{j,t}^{PV}+En_{j,t}^{ES}\right),\ \forall j\in\mathbf{V},\forall t \tag{21}$$

$$-Mc_{ij,t}\le F_{ij,t}^{G}\le Mc_{ij,t}\ ,\ \forall(i,j)\in\mathbf{L},\forall t \tag{22}$$

Constraint (21) represents the nodal power balance for the fictitious network. For the node with an energized controllable generator ($En_{j,t}^{G}=1$), the constraint for node *j* is relaxed, which means node *j* can be a fictitious power source and the power output is unlimited. Then the PV unit or ESS at the same connected graph can receive the fictitious power flow, i.e. the PV unit or ESS can be energized. Constraint (22) forces fictitious power flow on a disconnected line to be 0.

E. Repair Crew Dispatch and Operation Time Constraints

Fig. 5 shows an example of the routing path of a repair crew. After leaving the start point *SP*, it first travels to open a MS, then repairs fault components. If the carried resources are not enough to fix a component, the repair crew goes back to the depot to pick up resources. After faults are fixed, it closes the MS to reconnect the load island and finally returns to the return point *RP*.

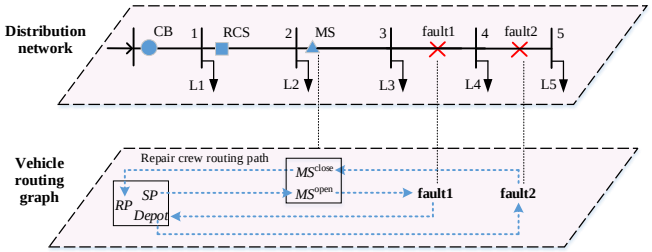

Fig. 5. Distribution network and repair crew routing path

The routing problem is defined in terms of a graph $G=\langle N,E\rangle$ where *N* represents the vertices containing the depots, MSs and damaged components. *E* represents the edges, i.e. the travel paths between two vertices.

For each MS, we set two vertices at the same location to represent a closed switch to be opened and an open switch to be closed by the repair crew. For example, the vertices in Fig. 5 are {*SP*, *MS*$^{\text{open}}$, *MS*$^{\text{close}}$, fault1, fault2, *depot*, *RP*}. In doing so, the repair crew can arrive at a MS twice to fulfill fault isolation and load island reconnection while satisfying the constraint that a vertex cannot be visited more than once, which is necessary for crew routing formulations based on the vehicle-routing problem (VRP). The crew routing and operation time constraints are:

$$\sum_{m\in\mathbf{N}\cup SP}X_{m,c,n}-\sum_{m\in\mathbf{N}\cup RP}X_{n,c,m}=0\ ,\ \forall n\in\mathbf{N},c\in Crew \tag{23}$$

$$\tau_{n,c}=\sum_{m\in\mathbf{N}\cup RP}X_{n,c,m}\ \ ,\forall n\in\mathbf{N},c\in Crew \tag{24}$$

$$-(1-X_{n,c,m})M\le t_{n,c}^{start}+t_{n,c}^{opera}+t_{n,c,m}^{travel}-t_{m,c}^{arrive}\le(1-X_{n,c,m})M \quad \forall n\in\mathbf{N}\cup SP,m\in\mathbf{N}\cup RP,c\in Crew \tag{25}$$

$$0\le t_{n,c}^{arrive}\le t_{n,c}^{start}\le M\tau_{n,c},\ \forall n\in\mathbf{N},\ \forall c\in Crew \tag{26}$$

$$t_{SP,c}^{start}=0\ ,\ \ \forall c\in Crew \tag{27}$$

$$\sum_{c\in Crew}\left(t_{n,c}^{start}+\tau_{n,c}t_{n,c}^{opera}\right)\le\sum_{t=1}^{T_h}t\cdot f_{ij\kappa,t}^{MS,open} \le\sum_{c\in Crew}\left(t_{n,c}^{start}+\tau_{n,c}t_{n,c}^{opera}\right)+1-\varepsilon\ ,\ \forall n\in MS^{open} \tag{28}$$

$$\sum_{c\in Crew}\left(t_{n,c}^{start}+\tau_{n,c}t_{n,c}^{opera}\right)\le\sum_{t=1}^{T_h}t\cdot f_{ij\kappa,t}^{MS,close} \le\sum_{c\in Crew}\left(t_{n,c}^{start}+\tau_{n,c}t_{n,c}^{opera}\right)+1-\varepsilon\ ,\ \forall n\in MS^{close} \tag{29}$$

$$\sum_{c\in Crew}\left(t_{n,c}^{start}+\tau_{n,c}t_{n,c}^{opera}\right)\le\sum_{t=1}^{T_h}t\cdot f_{ij,t}^{fix} \le\sum_{c\in Crew}\left(t_{n,c}^{start}+\tau_{n,c}t_{n,c}^{opera}\right)+1-\varepsilon\ ,\ \forall n\in DN \tag{30}$$

$$\sum_{t=1}^{T_h}f_{ij\kappa,t}^{MS,open}\le\sum_{c\in Crew}\tau_{n,c}\le1\ ,\forall n\in MS^{open},\ \kappa=1,2 \tag{31}$$

$$\sum_{t=1}^{T_h}f_{ij\kappa,t}^{MS,close}\le\sum_{c\in Crew}\tau_{n,c}\le1\ \ ,\forall n\in MS^{close},\ \kappa=1,2 \tag{32}$$

$$\sum_{t=1}^{T_h}f_{n,t}^{fix}\le\sum_{c\in Crew}\tau_{n,c}\le1\ \ ,\forall n\in DN \tag{33}$$

Constraint (23) ensures for each damaged component or MS, one repair crew arriving at it should also leave it. In constraint (24), variable $\tau_{n,c}$ is used to record whether crew *c* has repaired damaged component *n* or operated MS *n*. Constraint (25) indicates that for each crew, the time to start repairing damaged component *n* or operating MS *n* adding the repair/operation time of component/MS *m* and the traveling time between *n*, *m* is equal to the arrival time of *m*. Constraint (26) states the time to start repairing or operating *m* should be later than the arrival time of *m*. Moreover, if component/MS *n* is not visited by a crew, the start and arrival time for this crew at *n* is set as 0. Constraint (27) forces the start time at the start point to be 0. In constraint (28), $t\cdot f_{ij\kappa,t}^{MS,open}$ is the time when MS *n* is opened, where κ is 1 or 2 depending on the side at which the *n*th MS is deployed. $t\cdot f_{ij\kappa,t}^{MS,open}$ is restricted by the start time and operation time. Similarly, constraint (29) determines the time to have MS *n* closed. Constraint (30) determines the time when damaged component *n* is brought back to normal status. Constraint (31) means MS *n* can be opened only if it is visited by one repair crew. Moreover, at most one crew is permitted to participate in opening it. Constraints (32), (33) are similar to (31) and related with closing a MS and fixing a damaged component.

F. Resources pick up Constraints

If the carried resources are not enough to fix the rest of the damaged components, the repair crew returns to the depot to pick up resources. The resources pick up constraints are listed as follows [11]:

$$\sum_{\forall r}Cap_{r}^{R}E_{c,m,r}\le Cap_{c}^{C},\forall m\in\mathbf{N},\ c\in Crew \tag{34}$$

$$\sum_{n\in\mathbf{N}\cup SP}X_{n,c,m}\mathcal{R}_{m,r}\le E_{c,m,r},\forall m\in\mathbf{N},\ r,\ c\in Crew \tag{35}$$

$$-M\left(1-X_{m,c,n}\right)\le E_{c,m,r}-\mathcal{R}_{m,r}-E_{c,n,r}\le M\left(1-X_{m,c,n}\right) \quad \forall m\in\mathbf{N}\cup SP_c\setminus\{w\}\ ,n\in\mathbf{N}\cup RP_c\ ,c\in Crew,\ r \tag{36}$$

$$-M\left(1-X_{w,c,n}\right)\le E_{c,w,r}+Res_{c,w,r}^{C}-E_{c,n,r}\le M\left(1-X_{w,c,n}\right) \quad \forall w,\ n\in\mathbf{N},\ c\in Crew,\ r \tag{37}$$

$$-M\left(1-X_{SP_c,c,n}\right)\le Res_{c,SP_c,r}^{C}-E_{c,n,r}\le M\left(1-X_{SP_c,c,n}\right) \quad \forall n\in\mathbf{N}\cup RP_c,\ c\in Crew,\ r \tag{38}$$

Constraint (34) ensures that the amount of carried resources by one crew should be limited by the crew's capacity. Constraint (35) indicates that the crews can travel to a component only if they have enough resources to repair it. Constraint (36) ensures if a crew travels from component *m* to *n*, the resources that the crew has when arriving at *n* equals to the carried resources at *m* minus the required resources to repair

m. If a crew goes to depot *w* to pick up resources, the unit number of carried resources increases by $Res^{C}_{c,w,r}$, which is enforced by (37). Constraint (38) states the unit number of resources that the crew has at the first damaged component is equal to the initial resources obtained at the starting point.

G. Coupling Constraints

The statuses of switches and damaged components are altered by repair crews and DS operators, which is described as:

$$-\left(y^{RCS}_{ij\kappa}+y^{MS}_{ij\kappa}f^{MS,open}_{ij\kappa,t}\right)M \le y_{ij\kappa,t}-y_{ij\kappa,t-1} \le \left(y^{RCS}_{ij\kappa}+y^{MS}_{ij\kappa}f^{MS,close}_{ij\kappa,t}\right)M \quad \forall (i,j)\in \mathbf{L}, \forall t,\ \kappa=1,2 \tag{39}$$

$$Fix_{ij,t}=\sum_{t'=1}^{t'=t} f^{fix}_{ij,t'},\ \forall (i,j)\in L \tag{40}$$

Constraint (39) denotes the switch status can be changed at time step *t* if one of the following conditions is satisfied: 1) the switch is a RCS ($y^{RCS}_{ij\kappa}=1$) and 2) the switch is a MS ($y^{MS}_{ij\kappa}=1$) and the operation of the switch is completed by the repair crew at time step *t* ($f^{MS,open}_{ij\kappa,t}=1$ or $f^{MS,close}_{ij\kappa,t}=1$). In constraint (40), binary variable $Fix_{ij,t}$ denotes whether the damaged component has been fixed at time step *t*.

If damaged component *n* is found out by damage assessors ($f^{check}_{ij}=1$) and repaired by repair crews ($Fix_{ij,t}=1$), it returns to normal status ($B_{ij,t}=0$). Moreover, if a component hasn't been checked by assessors ($f^{check}_{ij}=0$), it is regarded as a potential damaged component ($B_{ij,t}=1$), which is constrained by (41).

$$1-B_{ij,t}=f^{check}_{ij}Fix_{ij,t},\ \forall (i,j)\in L,\ \forall t \tag{41}$$

For the definite non-fault components which don't need to be checked by damage assessors, parameter f^{check}_{ij} is set as 1.

H. Rolling Optimization for Service Restoration

The final form of the proposed service restoration model is as follows.

Objective: (1)

s.t. (2)-(41).

The terms of multiplication of binary variables such as $y_{ij2,t}B_{ij,t}$ and $y_{ij1,t}y_{ij2,t}x_{i,t}$ in constraints (15), (16) can be linearized to transform the model into a mixed-integer linear programming (MILP) problem. The linearization processes are represented by (42), (43).

$$z^{y_2B}_{ij}=y_{ij2,t}B_{ij,t},\ z^{y_2B}_{ij}\le y_{ij2,t},\ z^{y_2B}_{ij}\le B_{ij,t},\ z^{y_2B}_{ij}\ge y_{ij2,t}+B_{ij,t}-1 \tag{42}$$

$$\begin{cases} z^{yx}_{ij}=y_{ij1,t}y_{ij2,t}x_{i,t} \\ z^{yx}_{ij}\le y_{ij1,t},\ z^{yx}_{ij}\le y_{ij2,t},\ z^{yx}_{ij}\le x_{i,t},\ z^{yx}_{ij}\ge y_{ij1,t}+y_{ij2,t}+x_{i,t}-2 \end{cases} \tag{43}$$

The flowchart of the service restoration model coordinated with damage assessment is depicted in Fig. 6.

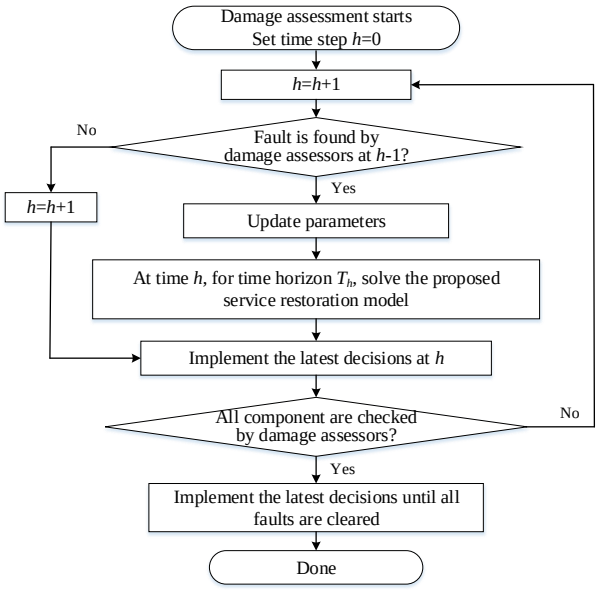

Fig. 6. Flowchart of the coordination mechanism

After damage assessment starts, at each time step, parameters are updated to initialize the model solution if new faults are revealed at the previous time step. The updated parameters include start point SP_c, damaged component set *DN*, line check status f^{check}_{ij}, initial switch status $y_{ij\kappa,0}$, carried resources at the start point $Res^{C}_{c,SP_c,r}$, required resources Res^{req}_{n}, remaining repair /operation time $t^{opera}_{n,c}$, travel time from the start point to each vertex $t^{travel}_{SP,c,n}$ and initial stored energy of ESS $E^{ES,ini}_{j}$. After the parameters update process, the proposed service restoration model is solved and the obtained restoration decisions are implemented at the current time step. If no fault is found out at the previous time step, the repair crews and system operators will proceed to implement the latest decisions. This procedure is repeated until all potential fault components are checked by damage assessors. After that the latest decisions will be carried on to complete the restoration.

The selection of time horizon T_h plays an important role in improving model performance. A shorter horizon could result in short-sighted decisions which may impede crews to fix the components requiring long repair time. On the other hand, selecting a longer horizon increases the deviation between input parameters and the uncertainties realization and also increases the computational burden. T_h can be determined via the following approach including 3 steps: 1) cluster the identified damaged components to each crew to minimize the largest time spent by crews in repairing all assigned components without considering the travel time; 2) obtain a feasible routing path of each crew to traverse and repair the assigned components considering resources pick up requirements; 3) calculate the time spent by each crew and set T_h slightly larger than the maximum time to allow possible switch operations.

IV. Case Study

The proposed model is first applied to a 70-node test system [28] to demonstrate the implementation process. Then it is applied to the IEEE 123-node system [29] to validate the model effectiveness. The problems are modeled in MATLAB and

This article has been accepted for publication in a future issue of this journal, but has not been fully edited. Content may change prior to final publication. Citation information: DOI 10.1109/TPWRS.2021.3137257, IEEE Transactions on Power Systems

solved by Gurobi 9.1.0 on a PC with Intel Core i7-6700 3.40 GHz CPU and 16 GB RAM. MIP gap of Gurobi is set as 0.5%.

Assume the damage assessment starts at 12:00 a.m. The duration of 1 time step is set as 15 min. Four types of resources are required to fix all the faults and the required capacities of one unit of the 4 types of resources are {3,2,5,2}. Maximum carrying capacity of each repair crew is 30. The carried unit number for the 4 types of resources at the start point of each crew is set as {3,3,1,3}. The operation time to open or close a MS is set as15 min.

A. 70-Node Test System

1) Test system and case design

The 70-node test system is shown in Fig. 7. It has 2 substations, 4 feeders, 70 nodes and 78 branches. The capacity of each substation is set as 5 MVA. The system has been modified by adding 4 CBs, 11 RCSs, 6 MSs, 4 dispatchable DGs rated at 500 kW / 250 kVAr, 1 PV rated at 50 kW and 1 ESS rated at 50 kW/200 kWh. The normalized profile of PV output is set according to Ref. [30]. The line capacity is 1.5 MVA. The load data can be found in [28]. Total load of the system is 4468kW.

Assume an extreme event caused 4 faults at line L68-69, L10-11, L18-19 and L32-39 respectively. The CBs at L1-2, L1-16 and L30-70 are triggered to interrupt the downstream feeders. The potential fault parts are divided as 3 areas (A1-A3) according to the damage assessors patrol progress, as shown in Fig. 7. At the end of each time step, one area is checked, i.e. damage assessment of A1-A3 is completed at 12:15, 12:30, 12:45. Three repair crews are deployed at the depot. The repair time of each damaged component is set as 1h. Required resources of damaged components are listed in Table I. Travel time between two vertices (the depot, damage components and MSs) is set in the range of 9~21min (0.6~1.4 time step).

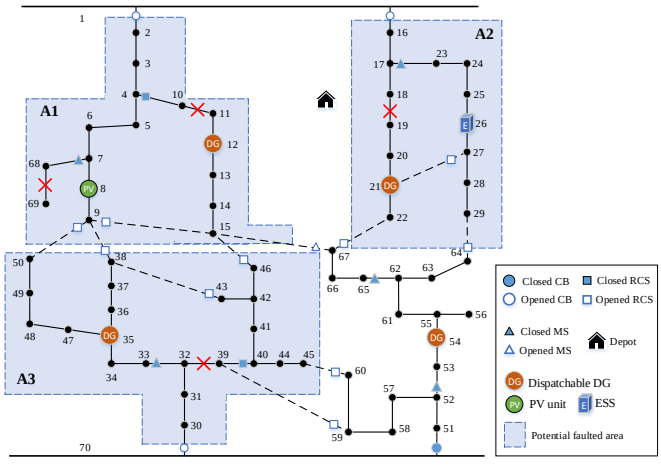

Fig. 7. Modified 70-node test system

TABLE I
REQUIRED RESOURCES OF DAMAGED COMPONENTS

Damaged component	L68-69	L10-11	L18-19	L32-39
Required units of resources (type A/B/C/D)	1/0/0/1	1/1/0/0	0/1/1/0	0/0/2/0

2) Numerical results

The service restoration starts at 12:15 and we set 12:15-12:30 as time step 1. The optimization is solved at the start of time step 1, 2, 3 respectively with time horizon T_h=10. The repair crew routing decisions are listed in Tables II-IV, where MSO denotes opening a MS and MSC denotes closing a MS. The bracket after an arrow notes the start and end of travel time while the bracket after a component/MS notes the start and end of operation time. The computational time for the 3 optimization problems is 32s, 153s and 290s, respectively.

TABLE II
REPAIR CREW ROUTING DECISION MADE AT TIME STEP 1

Crew 1	SP_1 → (12:15-12:27) **MSO7-68** (12:30-12:45) → (12:45-12:45) **MSC7-68** (13:30-13:45) →RP_1
Crew 2	SP_2 → (12:15-12:33) **L68-69** (12:45-13:45) →RP_2
Crew 3	SP_3 → (12:15-12:24) **L10-11** (12:30-13:30) →RP_3

TABLE III
REPAIR CREW ROUTING DECISION MADE AT TIME STEP 2

Crew 1	SP_1 → (12:30-12:30) **MSO7-68** (12:30-12:45) → (12:45-12:54) **L68-69** (13:00-14:00) →RP_1
Crew 2	SP_2 → (12:30-12:45) **MSO17-23** (12:45-13:00) → (13:00-13:09) **L18-19** (13:15-14:15) → RP_2
Crew 3	SP_3 → (12:30-12:30) **L10-11** (12:30-13:30) → (13:30-13:48) **MSC7-68**(14:00-14:15) → RP_3

TABLE IV
REPAIR CREW ROUTING DECISION MADE AT TIME STEP 3

Crew 1	SP_1 → (12:45-13:00) **MSO32-33** (13:00-13:15) →(13:15-13:36) **L18-19** (13:45-14:45)→RP_1
Crew 2	SP_2 → (12:45-12:45) **MSO17-23** (12:45-13:00) →(13:00-13:09)*depot*(13:09-13:09)→(13:09-13:30) **L32-39** (13:30-14:30) → (14:30-14:45) **MSC7-68** (14:45-15:00) →RP_2
Crew 3	SP_3 → (12:45-12:45) **L10-11** (12:45-13:30) → (13:30-13:45) **L68-69** (13:45-14:45) → RP_3

At the start of time step 1, potential faulted area A1 is checked and faults L68-69, L10-11 are identified, crew 1 is scheduled to open MS7-68 to restore load at node 2-9 and then close MS7-68 after fault L68-69 is repaired to restore load 68 and 69. Crew 2, 3 are scheduled to repair the two faults. At the start of time step 2, crews 1, 3 arrive at their targets while crew 2 is on the way to fault L68-69. Area A2 is checked and fault L18-19 is found. The optimal dispatch decision is updated. Crew 1 starts to open MS7-68 and crew 3 starts to repair L10-11. Crew 2 is dispatched to travel to MS17-23. At the start of time step 3, all potential faulted areas are checked and the final routing decision is updated as shown in Table IV. It can be seen by this moment, MS7-68 has been opened by crew 1 and the repair of L10-11 by crew 3 has lasted for 15 mins. The required resources of fault L32-39 is beyond the hold of crew 2, so the crew is dispatched to pick up resources from the depot before repairing L32-39.

All loads are restored at 15:00. The switch operation, fault repair and load restoration in actual execution are shown in Table V. It can be seen that an increase in served load usually results from fault isolation, fault repair and island reconnection.

TABLE V
SWITCH OPERATION, FAULT REPAIR AND LOAD RESTORATION IN ACTUAL EXECUTION

Time (End of time step #)	Fault location	MS/CB/RCS operation	Fault brought to normal status	Served load (kW)
12:15 (0)	L68-69, L10-11			\
12:30 (1)	L18-19	open RCS4-10		1244
12:45 (2)	L32-39	open MS7-68, close CB1-2		1691
13:00 (3)		open RCS39-40, MS17-23 close RCS29-64, RCS45-60		2497
13:15 (4)		open RCS45-60, MS32-33, close RCS9-50, RCS38-43		3471
13:30 (5)		close RCS15-46	L10-11	3727
13:45 (6)				3727
14:00 (7)				3727
14:15 (8)				3727
14:30 (9)		close CB30-70	L32-39	4030
14:45 (10)		close CB1-16	L68-69, L18-19	4328
15:00 (11)		close MS7-68		4468

Fig. 8 shows the reconfiguration and load restoration results at13:00 and 15:00. After opening MS17-23, RCS39-40 and closing RCS29-64, RCS45-60 before 13:00, the faults at L18-19 and L32-39 are isolated, then load 23-29, 40-46 is energized

This article has been accepted for publication in a future issue of this journal, but has not been fully edited. Content may change prior to final publication. Citation information: DOI 10.1109/TPWRS.2021.3137257, IEEE Transactions on Power Systems

by substation 70 together with DG 54 and ESS 26, as shown in Fig. 8 (a). After faults are cleared, the isolated parts such as nodes 68 and 69 can be reconnected, as shown in Fig. 8 (b).

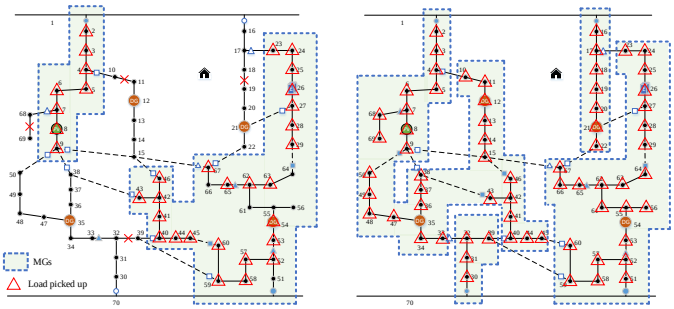

(a) 13:00 (b) 15:00

Fig. 8. Reconfiguration and load restoration results at 13:00 and 15:00

B. 123-Node Test System

1) Test system and case design

As shown in Fig. 9, the modified IEEE 123-node system has 1 substation with the capacity of 5MVA. There are 6 dispatchable DGs, 2 PV units and 1 ESS. Parameters of DERs are set the same as the 70-node test system in Section IV.A. 3 CBs, 6 RCSs and 6 MSs are added. Five faults occur at line L64-65, L67-119, L52-118. L93-94 and L108-109. The CB at L13-118 is opened to interrupt the downstream network. The potential fault parts A1-A4 are checked at 12:15, 12:30, 12:45 and 13:00. 2 repair crews are deployed at depot 1 and 1 repair crew is deployed at depot 2. The required repair time and resources of damaged components are shown in Table VI. Travel time between two vertices is set in range of 15~30min.

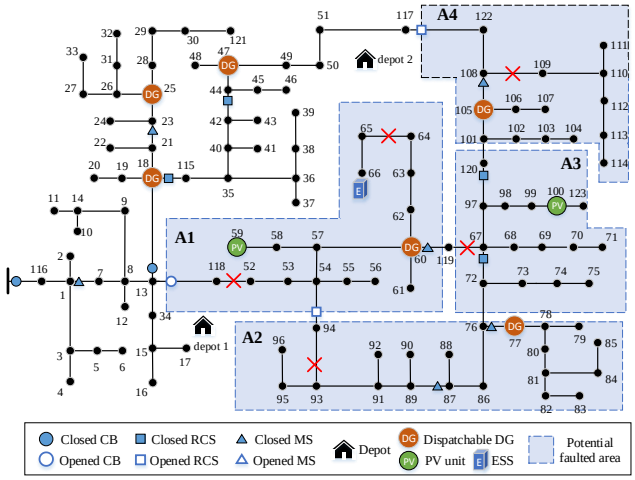

Fig. 9. Modified 123-node test system

TABLE VI
REQUIRED RESOURCES OF DAMAGED COMPONENTS

Damaged component	L64-65	L67-119	L52-118	L93-94	L108-109
Repair time	1h	1h	1h	1.5h	1.5h
Required units of resources (type A/B/C/D)	1/0/0/1	1/1/0/0	0/1/1/0	0/2/0/1	0/0/2/0

2) Effect of coordinating with damage assessment

To show the effect of restoration in coordination with damage assessment, the following 3 cases are compared:

Case 1: the proposed model.

Case 2: service restoration is conducted after damage assessment of the whole system is completed.

Case 3: isolation is performed during damage assessment to divide the potential faulted areas into multiple node cells, i.e. groups of system components interconnected by non-switchable lines [12]. Then service restoration is implemented after damage assessment of the whole system is done.

In case 3, the time spent on the damage assessment stage is assumed to be 90 mins. The additional 30 mins are spent in opening all MSs in the potential faulted areas. In both cases 2 and 3, the intimal carried resources of each crew are adjusted and the crews don't need to go back to replenish resources since the restoration decisions are made after all faults are assessed.

The repair crew dispatch of the 3 cases starts at 12:15, 13:00 and 13:30 respectively. The crew routing paths of the 3 cases are sketched in Fig. 10. A difference between the routing paths can be observed. In Fig. 10 (a), the routing path for case 1 generally extends as damage assessment progresses. In Fig. 10 (b), since all faults are explicit, the repair crews follow a globally optimal routing path. In both cases, MS87-89 is opened earlier because it is an important step to isolate faults and restore load 72-88. In Fig. 9 (c), the crews are mainly dispatched to repair damaged components because fault isolation is done beforehand. The detailed fault repair and switching timetable is shown in Table VII. It can be seen that restoration of case 1 is finished 30 mins earlier than the other 2 cases.

The load and energy restoration results of the 3 cases are presented in Figs. 11 and 12. The restored load curve of case 1 is highest in most time steps. Total served energy of case 1 during 12:15-16:30 is 11715 kWh, which is 7.5% higher than the value of case 2, i.e., 10901 kWh, and 13.8% higher than case 3, i.e., 10290 kWh. It can be concluded that through coordinating restoration with damage assessment, the restoration effect is notably improved and restoration time is reduced. Moreover, restoration effect of case 2 is slightly superior to that of case 3 because the non-optimal preliminary isolation postpones the start of fault repair.

TABLE VII
FAULT REPAIR AND SWITCH OPERATION TIMETABLE OF CASE 1-3

Time (End of time step #)	Case 1	Case 2	Case 3
13:15 (4)	open MS87-89, RCS97-120, RCS67-72		
13:30 (5)	repair L52-118, L64-65	open MS87-89, MS105-108, RCS67-72, RCS97-120	open all switches in faulted areas
13:45 (6)	open MS60-119 close CB13-118		
14:00 (7)	open MS105-108		
14:15 (8)			close RCS54-94
14:45 (10)	repair L93-94 close RCS54-94	repair L52-118, L64-65	repair L93-94, L52-118, L64-65 close CB13-118
15:00 (11)		repair L67-119 close RCS67-72, RCS97-120, CB13-118	
15:15 (12)	close MS87-89		close MS87-89
15:30 (13)	repair L67-119 close RCS67-72, RCS97-120		
16:00 (15)	repair L108-109 close RCS117-122	repair L93-94 close RCS54-94	
16:30 (17)		repair L108-109 close RCS117-122	repair L67-119, L108-109 close RCS67-72, RCS97-120, RCS117-122

This article has been accepted for publication in a future issue of this journal, but has not been fully edited. Content may change prior to final publication. Citation information: DOI 10.1109/TPWRS.2021.3137257, IEEE Transactions on Power Systems

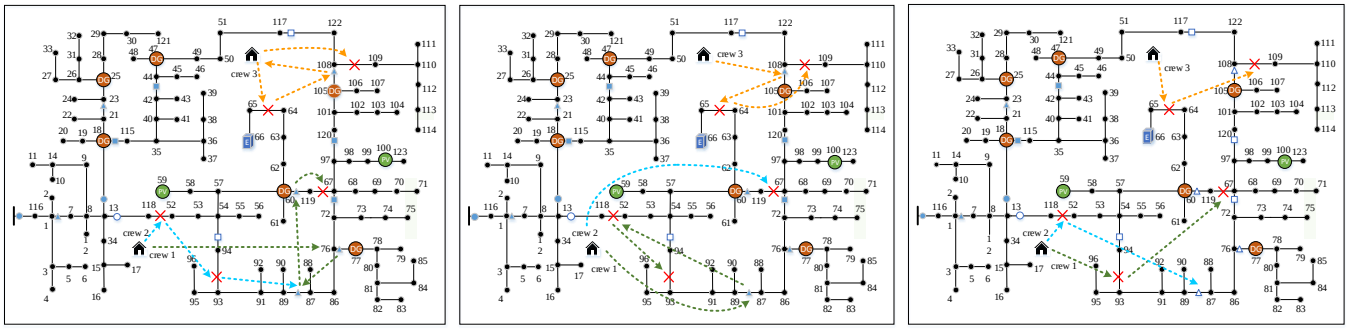

(a) Case 1 (b) Case 2 (c) Case 3

Fig. 10. Repair crew routing paths of 3 cases

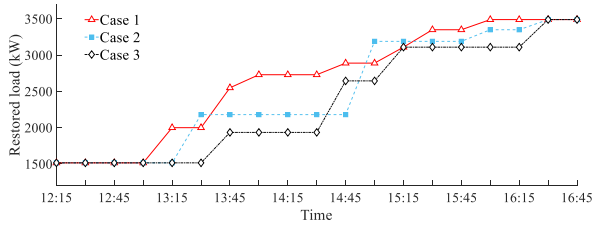

Fig. 11. Load restoration results of 3 cases

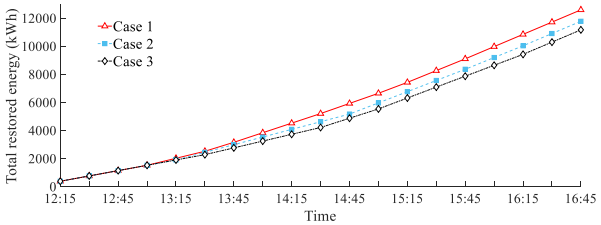

Fig. 12. Energy restoration results of 3 cases

3) Impact of component repair time

The variation of fault repair time may affect the crew dispatch decision and restoration efficiency. To analyze the influence, we adopt a parameter *RT*, which ranges from 0.5 to 2, as the multiplier of base repair time shown in Table VI for each damaged component. Table VIII shows the sequences of MS operation / fault repair completion time under *RT*=0.5, 1, 1.5 and 2.

TABLE VIII
ACTION SEQUENCE UNDER DIFFERENT REPAIR TIME

Order of actions	1	2	3	4	5	6	7	8
RT=0.5	MS60-119	L52-118 L64-65	MS105-108	L93-94	L67-119	L108-109		
RT =1	MS87-89	L52-118 L64-65	MS60-119	MS105-108	L93-94	MSC87-89	L67-119	L108-109
RT =1.5	MS87-89	MS60-119	L52-118 L64-65	MS105-108	MSC87-89	L93-94	L67-119	L108-109
RT =2	MS87-89	MS105-108	L52-118 L64-65 MS60-119	L93-94	MSC87-89	L67-119	L108-109	

As *RT* increases, the MS operation sequence changes obviously. When *RT*=0.5, crews only need to open MS60-119 and MS105-108 because faults will be cleared within a short time and isolating is not a priority. Moreover, as *RT* varies from 1.5 to 2, the operation of MS60-119 is postponed. It is because repairing faults L52-118, L64-65 and L67-119 will take a lot of time and opening MS60-119 before {L52-118, L64-65} or L67-119 is repaired is not helpful for load restoration. The load restoration curves under *RT*=0.5, 1, 1.5, 2 are compared in Figs. 13. It can be seen that the restoration efficiency is highly dependent on component repair time.

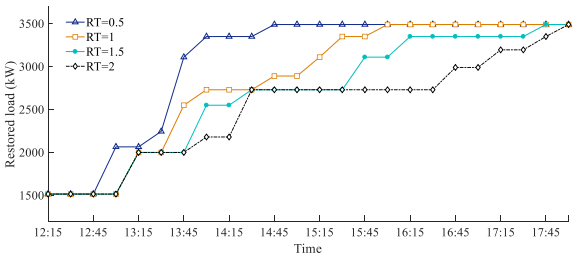

Fig. 13. Load restoration results under *RT*=0.5, 1, 1.5, 2

To further investigate the impact of component repair time, we compare the influence of repair time variation on the effectiveness of different restoration strategies. The 3 cases designed before is simulated with *RT*=0.5, 1, 1.5 and 2. Total curtailed energy for the cases during the restoration process is shown in Fig. 14.

Fig. 14. Total curtailed energy of 3 cases under *RT*=0.5, 1, 1.5, 2

It can be seen that under all values of *RT*, case 1 is always ahead of the others in restoration performance, which validates the effectiveness of the proposed model once again. In addition, as repair time increases, the difference between the effect of case 1 and the other cases is gradually reduced. An important reason is that coordinating with damage assessment allows crews to repair some components earlier, nevertheless repairing these components first may not be the optimal decision had the DS operators obtained the global damage status information.

V. DISCUSSION AND CONCLUSION

This paper proposed an optimal DS restoration model considering the coordination with damage assessment. The restoration measures including fault isolation, reconfiguration, fault repair and network reconnection were integrated. The restoration schedule was updated as damage assessment progresses. Constraints describing the relationship between fault location, switch status and node status were formulated to

obtain the optimal switching and crew dispatch decisions. Numerical studies demonstrated the effectiveness of the coordination mechanism.

An important issue in DS restoration is the uncertainties of load, renewable power generation and repair time. To obtain high-quality and accurate solutions, there is a need to improve the proposed model by characterizing the uncertainties and developing effective algorithms. Moreover, demand response technologies have great potential to mitigate power outage losses. In addition, in future work, it is meaningful to improve the model by considering the three-phase unbalanced operation of DS.

APPENDIX

This appendix provides the description of the completeness of constraints (15)-(18) in determining the exact status of each node in the network if switches statuses and the locations of multiple faults are given.

Take line (*i*, *j*) affecting node *j* as an example, the description is as follows. Define a three-dimensional array (*a*, *b*, *c*), where *a* can be 0, 1, 2 or 3. *a*=0 denotes the switches at both sides of line (*i*, *j*) are opened. *a*=1 denotes the switch at *i* side of line (*i*, *j*) is opened while the switch at *j* side is closed or there is no switch at *j* side. Contrarily, *a*=2 denotes only the switch at *j* side of line (*i*, *j*) is opened. *a*=3 denotes the switch at each side of line (*i*, *j*) is closed or no switch exists at the side. *b* can be 0 or 1. If line (*i*, *j*) is faulted, *b*=1. Otherwise *b*=0. *c* can be 0 or 1. If node *i* is influenced by outage propagation, *c*=1, or *c*=0. Array (*a*, *b*, *c*) has 16 possible values, representing all possible status of line (*i*, *j*) and node *i*. The inclusion of these status in scenarios A to E is shown in Table A1.

TABLE B1
LINE STATUS INCLUDED IN SCENARIOS A-E

A: (1,1,0), (1,1,1), (3,1,0), (3,1,1)	**A∪B**: (1,1,0), (1,1,1), (3,1,0), (3,0,1), (3,1,1)
B: (3,0,1), (3,1,1)	
C: (0,0,0), (0,0,1), (0,1,0), (0,1,1), (2,0,0), (2,0,1), (2,1,0), (2,1,1)	**C∪D∪E**: (0,0,0), (0,0,1), (0,1,0), (0,1,1), (1,0,0), (1,0,1), (2,0,0), (2,0,1), (2,1,0), (2,1,1), (3,0,0)
D: (0,0,0), (0,0,1), (1,0,0), (1,0,1)	
E: (0,0,0), (1,0,0), (2,0,0), (3,0,0)	

It can be seen that A∪B and C∪D∪E are complementary events and 5 scenarios include all possible ways in which power outage affects node *j* through line (*i*, *j*). Since Table A1 is applicable to describe the influence of any connected line on node *j*, the completeness of scenarios A to E and the corresponding constraints is proved.

VI. REFERENCES

[1] M. Panteli and P. Mancarella, "The grid: Stronger, bigger, smarter?: Presenting a conceptual framework of power system resilience," *IEEE Power Energy Mag.*, vol. 13, no. 3, pp. 58–66, May/Jun. 2015.

[2] Z. Bie, Y. Lin, G. Li and F. Li, "Battling the Extreme: A Study on the Power System Resilience," *Proceedings of the IEEE*, vol. 105, no. 7, pp. 1253-1266, July 2017.

[3] J. Li, X. Ma, C. Liu and K. P. Schneider, "Distribution System Restoration With Microgrids Using Spanning Tree Search," *IEEE Transactions on Power Systems*, vol. 29, no. 6, pp. 3021-3029, Nov. 2014

[4] C. Chen, J. Wang, F. Qiu and D. Zhao, "Resilient Distribution System by Microgrids Formation After Natural Disasters," *IEEE Transactions on Smart Grid*, vol. 7, no. 2, pp. 958-966, March 2016.

[5] Y. Xu, C. Liu, K. P. Schneider, F. K. Tuffner and D. T. Ton, "Microgrids for Service Restoration to Critical Load in a Resilient Distribution System," *IEEE Transactions on Smart Grid*, vol. 9, no. 1, pp. 426-437, Jan. 2018.

[6] B. Chen, C. Chen, J. Wang and K. L. Butler-Purry, "Sequential Service Restoration for Unbalanced Distribution Systems and Microgrids," *IEEE Transactions on Power Systems*, vol. 33, no. 2, pp. 1507-1520, March 2018

[7] A. Arif, Z. Wang, J. Wang and C. Chen, "Power Distribution System Outage Management With Co-Optimization of Repairs, Reconfiguration, and DG Dispatch," *IEEE Transactions on Smart Grid*, vol. 9, no. 5, pp. 4109-4118, Sept. 2018

[8] S. Lei, C. Chen, Y. Li and Y. Hou, "Resilient Disaster Recovery Logistics of Distribution Systems: Co-Optimize Service Restoration With Repair Crew and Mobile Power Source Dispatch," *IEEE Transactions on Smart Grid*, vol. 10, no. 6, pp. 6187-6202, Nov. 2019.

[9] M. Farajollahi, M. Fotuhi-Firuzabad and A. Safdarian, "Optimal Placement of Sectionalizing Switch Considering Switch Malfunction Probability," *IEEE Transactions on Smart Grid*, vol. 10, no. 1, pp. 403-413, Jan. 2019.

[10] S. Ma, S. Li, Z. Wang and F. Qiu, "Resilience-Oriented Design of Distribution Systems," *IEEE Transactions on Power Systems*, vol. 34, no. 4, pp. 2880-2891, July 2019.

[11] A. Arif, Z. Wang, C. Chen and J. Wang, "Repair and Resource Scheduling in Unbalanced Distribution Systems Using Neighborhood Search," *IEEE Transactions on Smart Grid*, vol. 11, no. 1, pp. 673-685, Jan. 2020.

[12] B. Chen, Z. Ye, C. Chen, J. Wang, T. Ding and Z. Bie, "Toward a Synthetic Model for Distribution System Restoration and Crew Dispatch," *IEEE Transactions on Power Systems*, vol. 34, no. 3, pp. 2228-2239, May 2019.

[13] C. Chen, J. Wang and D. Ton, "Modernizing Distribution System Restoration to Achieve Grid Resiliency Against Extreme Weather Events: An Integrated Solution," *Proceedings of the IEEE*, vol. 105, no. 7, pp. 1267-1288, July 2017

[14] M. Farajollahi, M. Fotuhi-Firuzabad and A. Safdarian, "Simultaneous Placement of Fault Indicator and Sectionalizing Switch in Distribution Networks," *IEEE Transactions on Smart Grid*, vol. 10, no. 2, pp. 2278-2287, March 2019.

[15] Y. Jiang, C. Liu, M. Diedesch, E. Lee and A. K. Srivastava, "Outage Management of Distribution Systems Incorporating Information From Smart Meters," *IEEE Transactions on Power Systems*, vol. 31, no. 5, pp. 4144-4154, Sept. 2016

[16] K. Sun, Q. Chen and Z. Gao, "An Automatic Faulted Line Section Location Method for Electric Power Distribution Systems Based on Multisource Information," *IEEE Transactions on Power Delivery*, vol. 31, no. 4, pp. 1542-1551, Aug. 2016.

[17] L. A. Freeman, G. J. Stano, and M. E. Gordon, "Best practices for storm responseon U.S. distribution systems," Distrib. Syst. Test. Appl. Res., Tampa, FL, USA, Tech. Rep., Mar. 2010.

[18] P. Van Hentenryck, N. Gillani and C. Coffrin, "Joint assessment and restoration of power systems", Proc. 20th Euro. Conf. Artif. Intell. Appl., pp. 792-797, Aug. 2012.

[19] K. Lian, Z. Chen, J. Wu and W. Fu, "Practice of Emergency Response Mechanism for Large Blackout in Power Supply Enterprises," (in Chinese), *Electric Safety Technology*, vol. 23, no. 01, pp. 1–4, 2021.

[20] S. Lei, J. Wang and Y. Hou, "Remote-Controlled Switch Allocation Enabling Prompt Restoration of Distribution Systems," *IEEE Transactions on Power Systems*, vol. 33, no. 3, pp. 3129-3142, May 2018.

[21] M. Lwin, J. Guo, N. Dimitrov and S. Santoso, "Protective Device and Switch Allocation for Reliability Optimization With Distributed Generators," *IEEE Transactions on Sustainable Energy*, vol. 10, no. 1, pp. 449-458, Jan. 2019.

[22] G. J. Lim, S. Kim, J. Cho, Y. Gong and A. Khodaei, "Multi-UAV Pre-Positioning and Routing for Power Network Damage Assessment," *IEEE Transactions on Smart Grid*, vol. 9, no. 4, pp. 3643-3651, July 2018.

[23] M. E. Baran and F. F. Wu, "Network reconfiguration in distribution systems for loss reduction and load balancing," *IEEE Transactions on Power Delivery*, vol. 4, no. 2, pp. 1401-1407, April 1989.

[24] Z. Ye, C. Chen, B. Chen and K. Wu, "Resilient Service Restoration for Unbalanced Distribution Systems With Distributed Energy Resources by Leveraging Mobile Generators," *IEEE Transactions on Industrial Informatics*, vol. 17, no. 2, pp. 1386-1396, Feb. 2021.

[25] T. Ding, Y. Lin, G. Li and Z. Bie, "A New Model for Resilient Distribution Systems by Microgrids Formation," *IEEE Transactions on Power Systems*, vol. 32, no. 5, pp. 4145-4147, Sept. 2017

[26] Y. Lin, B. Chen, J. Wang and Z. Bie, "A Combined Repair Crew Dispatch Problem for Resilient Electric and Natural Gas System Considering Reconfiguration and DG Islanding," *IEEE Transactions on Power Systems*, vol. 34, no. 4, pp. 2755-2767, July 2019.

[27] T. Ding, Y. Lin, Z. Bie and C. Chen, "A resilient microgrid formation strategy for load restoration considering master-slave distributed generators and topology reconfiguration," *Applied Energy*, vol. 199, pp. 205-216, May. 2017.
[28] D. Das, "A fuzzy multiobjective approach for network reconfiguration of distribution systems," *IEEE Transactions on Power Delivery*, vol. 21, no. 1, pp. 202-209, Jan. 2006
[29] IEEE PES AMPS DSAS Test Feeder Working Group. (Feb. 3, 2014). 123-Bus Feeder. Accessed: May 12, 2018. [Online]. Available: http://sites.ieee.org/pes-testfeeders/resources/
[30] M. R. Dorostkar-Ghamsari, M. Fotuhi-Firuzabad, M. Lehtonen and A. Safdarian, "Value of Distribution Network Reconfiguration in Presence of Renewable Energy Resources," *IEEE Transactions on Power Systems*, vol. 31, no. 3, pp. 1879-1888, May 2016.

Yiheng Bian (S'18) received the B.S. degree in electrical engineering from North China Electric Power University, Baoding, China, in 2017. Currently, he is pursuing the Ph.D degree at Xi'an Jiaotong University, Xi'an, China. His major research interests include planning and operation of resilient power systems.

Chen Chen (Senior Member, IEEE) received the B.S. and M.S. degrees from Xi'an Jiaotong University (XJTU), Xi'an, China, in 2006 and 2009, respectively, and the Ph.D. degree in electrical engineering from Lehigh University, Bethlehem, PA, USA, in 2013.

He is currently a Professor with the School of Electrical Engineering, XJTU. Prior to joining XJTU, he has over six-year service with Argonne National Laboratory, Lemont, IL, USA, with the last appointment as Energy Systems Scientist with Energy Systems Division. His research interest includes power system resilience, distribution systems and microgrids, demand side management, communications and signal processing for smart grid. He is also the recipient of the IEEE PES Chicago Chapter Outstanding Engineer Award in 2017. He is an Editor of the IEEE Transactions on Smart Grid and IEEE Power Engineering Letters.

Yuxiong Huang (S'17) received the B.S. degree in electrical engineering from Xi'an Jiaotong University, Xi'an, China, in 2017, where he is currently pursuing the Ph.D degree. His major research interests include reliability evaluation and machine learning technologies in power systems.

Zhaohong Bie (Senior Member, IEEE) received the B.S. and M.S. degrees in Electric Power from Shandong University, Jinan, China, in 1992 and 1994, respectively, and the Ph.D. degree in Electrical Engineering from Xi'an Jiaotong University, Xi'an, China, in 1998. She is currently a Professor with the State Key Laboratory of Electrical Insulation and Power Equipment and the School of Electrical Engineering, Xi'an Jiaotong University. Her research interests include power system planning and reliability evaluation, integration of renewable energy, as well as the Energy Internet.

João P. S. Catalão (Senior Member, IEEE) received the M.Sc. degree from the Instituto Superior Técnico (IST), Lisbon, Portugal, in 2003, and the Ph.D. degree and Habilitation for Full Professor ("Agregação") from the University of Beira Interior (UBI), Covilha, Portugal, in 2007 and 2013, respectively. Currently, he is a Professor at the Faculty of Engineering of the University of Porto (FEUP), Porto, Portugal, and Research Coordinator at INESC TEC. He was the Primary Coordinator of the EU-funded FP7 project SiNGULAR ("Smart and Sustainable Insular Electricity Grids Under Large-Scale Renewable Integration"), a 5.2-million-euro project involving 11 industry partners. His research interests include power system operations and planning, power system economics and electricity markets, distributed renewable generation, demand response, smart grid, and multi-energy carriers.